

Phosphodiesterase 2A Localized in the Spinal Cord Contributes to Inflammatory Pain Processing

Wiebke Kallenborn-Gerhardt, Ph.D., Ruirui Lu, M.D., Aaron Bothe, M.D., Dominique Thomas, M.Sc., Jessica Schlaudraff, Ph.D., Jana E. Lorenz, M.Sc., Nancy Lippold, M.Sc., Catherine I. Real, M.Sc., Nerea Ferreirós, Ph.D., Gerd Geisslinger, M.D., Ph.D., Domenico Del Turco, Ph.D., Achim Schmidtke, M.D., Ph.D.

ABSTRACT

Background: Phosphodiesterase 2A (PDE2A) is an evolutionarily conserved enzyme that catalyzes the degradation of the cyclic nucleotides, cyclic adenosine monophosphate, and/or cyclic guanosine monophosphate. Recent studies reported the expression of PDE2A in the dorsal horn of the spinal cord, pointing to a potential contribution to the processing of pain. However, the functions of PDE2A in spinal pain processing *in vivo* remained elusive.

Methods: Immunohistochemistry, laser microdissection, and quantitative real-time reverse transcription polymerase chain reaction experiments were performed to characterize the localization and regulation of PDE2A protein and messenger RNA in the mouse spinal cord. Effects of the selective PDE2A inhibitor, BAY 60–7550 (Cayman Chemical, Ann Arbor, MI), in animal models of inflammatory pain (n = 6 to 10), neuropathic pain (n = 5 to 6), and after intrathecal injection of cyclic nucleotides (n = 6 to 8) were examined. Also, cyclic adenosine monophosphate and cyclic guanosine monophosphate levels in spinal cord tissues were measured by liquid chromatography tandem mass spectrometry.

Results: The authors here demonstrate that PDE2A is distinctly expressed in neurons of the superficial dorsal horn of the spinal cord, and that its spinal expression is upregulated in response to hind paw inflammation. Administration of the selective PDE2A inhibitor, BAY 60–7550, increased the nociceptive behavior of mice in animal models of inflammatory pain. Moreover, BAY 60–7550 increased the pain hypersensitivity induced by intrathecal delivery of cyclic adenosine monophosphate, but not of cyclic guanosine monophosphate, and it increased the cyclic adenosine monophosphate levels in spinal cord tissues.

Conclusion: Our findings indicate that PDE2A contributes to the processing of inflammatory pain in the spinal cord. (ANESTHESIOLOGY 2014; 121:372-82)

TISSUE injury and inflammation lead to a sensitization of the nociceptive system, resulting in increased responsiveness to noxious stimulation (hyperalgesia), pain evoked by normally innocuous stimuli (allodynia), and spontaneous pain.¹ Among the key second messengers of pain sensitization are the cyclic nucleotides, cyclic adenosine monophosphate (cAMP), and cyclic guanosine monophosphate (cGMP). Various downstream signaling mechanisms have been identified that mediate their pain-relevant functions, including activation of cAMP-dependent protein kinase,^{2–5} exchange protein directly activated by cAMP,^{6,7} cGMP-dependent protein kinase,^{8–11} cyclic nucleotide-gated channels,¹² and modulation of hyperpolarization-activated cyclic nucleotide-gated channels.¹³ Depending on the localization of generators and downstream signaling mechanisms, cGMP may exert both pronociceptive and antinociceptive functions,^{12,14} whereas increased cAMP levels seem to be generally associated with increased nociception.¹⁵

What We Already Know about This Topic

- Tissue injury leads to sensitization of pain pathways, and generation of cyclic adenosine monophosphate and cyclic guanosine monophosphate contributes to the development of sensitization.
- Little is known about the role of phosphodiesterases, enzymes that degrade these cyclic nucleotides, in experimental models of pain.

What This Article Tells Us That Is New

- Phosphodiesterase 2A expression was increased in the dorsal horn of mice after paw inflammation. Inhibition of phosphodiesterase 2A exacerbated nociceptive behavior with inflammatory but not with neuropathic pain.
- Inhibitors of phosphodiesterases, which are being developed for treatment of neuropsychiatric diseases, may increase pain perception.

The importance of cyclic nucleotides for pain sensitization requires a tight control of their intracellular

The first two authors contributed equally to this work (W.K.-G. and R.L.).

Submitted for publication July 23, 2013. Accepted for publication March 17, 2014. From the Pharmazentrum Frankfurt/Zentrum für Arzneimittelforschung, -entwicklung und -sicherheit, Institut für Klinische Pharmakologie, Universitätsklinikum Frankfurt, Frankfurt am Main, Germany (W.K.-G., R.L., A.B., D.T., J.E.L., N.L., N.F., G.G., A.S.); Institut für Pharmakologie und Toxikologie, Zentrum für Biomedizinische Ausbildung und Forschung, Universität Witten/Herdecke, Witten, Germany (R.L., C.I.R., A.S.); and Institut für Klinische Neuroanatomie, Neuroscience Center, Goethe-Universität, Frankfurt am Main, Germany (J.S., D.D.T.). Current address: Institut für Neuroradiologie, Universitätsklinikum Frankfurt, Frankfurt am Main, Germany (A.B.).

Copyright © 2014, the American Society of Anesthesiologists, Inc. Lippincott Williams & Wilkins. Anesthesiology 2014; 121:372-82

concentration. The enzymes responsible for breakdown of cAMP and cGMP are the cyclic nucleotide phosphodiesterases (PDEs). Twenty-one PDE genes have been identified, which are classified into 11 families (PDE1 to PDE11), each with distinct substrate specificity, regulatory properties, and tissue distribution.¹⁶ In contrast to many other physiological and pathophysiological processes, there is only little information available about the PDEs that are involved in pain processing. Interestingly, recent immunohistological studies detected the PDE isoform, PDE2A, in the dorsal horn of the spinal cord,¹⁷ pointing to potential pain-relevant functions of this enzyme. PDE2A is a dual-substrate PDE that can regulate either cAMP or cGMP levels, depending on the cell type in which it is expressed.¹⁸ Here, we aimed to elucidate whether PDE2A is functionally involved in pain processing, and whether its function is linked to cAMP and/or cGMP.

Materials and Methods

Animals

All experiments were approved by the federal authority for animal research (Regierungspräsidium, Darmstadt, Germany) and were performed in accordance with the National Institutes of Health's Guide for the Care and Use of Laboratory Animals. Experiments were performed in 6- to 8-week-old male C57BL/6N mice (Harlan, Venray, The Netherlands). Animals were housed on a 12/12 h light/dark cycle with standard rodent chow and water available *ad libitum*.

Behavioral Testing

The behavioral tests were performed blinded to treatment. The PDE2A inhibitor, BAY 60–7550 (Cayman Chemical, Ann Arbor, MI), which shows 50-fold selectivity for PDE2A compared with PDE1 and greater than 100-fold selectivity compared with the other PDEs,¹⁹ was dissolved in 100% ethanol and further diluted in ethanol:Kolliphor:H₂O-5:10:85 (for formalin test) or in ethanol:olive oil-11:89 (for all other experiments).

Formalin Test. Formalin (15 μ l of a 5% formaldehyde solution) was injected subcutaneously into the dorsal site of a hind paw, and the time spent licking the paw was recorded.²⁰

Zyosan-induced Hypersensitivity. A zyosan suspension (15 μ l, 5 mg/ml in 0.1 M phosphate buffered saline [PBS], pH 7.4; Sigma-Aldrich, Munich, Germany) was injected into the plantar subcutaneous space of a hind paw. Paw-withdrawal latency after mechanical stimulation was measured using a Dynamic Plantar Aesthesiometer (Ugo Basile, Comerio, Italy). This device pushes a thin probe (0.5 mm diameter) with increasing force through a wire-grated floor against the plantar surface of the paw from beneath, and it automatically stops and records the latency time at which the animal withdraws the paw.^{12,21,22} Paw-withdrawal latency after thermal stimulation was measured using a Plantar Analgesia Meter (model 390G; IITC, Woodland Hills, CA).

The latency time was calculated as the average of three to five consecutive exposures with at least 20 s in-between.

Acute Nociceptive Behavior. Paw-withdrawal latencies after mechanical and thermal stimulations were measured using the Dynamic Plantar Aesthesiometer and Plantar Analgesia Meter, respectively.

Intrathecal Drug Administration. Intrathecal delivery of drugs was performed by direct lumbar puncture in awake, conscious mice as described in detail.²² The cyclic nucleotides, cAMP, Sp-8-Br-cAMPS, cGMP (Biolog, Bremen, Germany), or the nitric oxide donor NOC-5 (Calbiochem/EMD Millipore, Darmstadt, Germany), were dissolved in sterile 0.9% NaCl and were administered in a volume of 5 μ l. Paw-withdrawal latencies were measured using the Dynamic Plantar Aesthesiometer.

Neuropathic Pain. The spared nerve injury (SNI) model²³ was used to investigate neuropathic pain behavior. Two branches of the sciatic nerve were ligated and cut distally, leaving the sural nerve intact. Paw-withdrawal latencies were measured using the Dynamic Plantar Aesthesiometer.

Immunostaining

Immunostainings were performed as described.²¹ Briefly, mice were perfused with 4% paraformaldehyde in PBS (pH 7.4), and lumbar dorsal root ganglia (DRGs; L4-L5) and spinal cords (L4-L5) were dissected, postfixed for 10 min in the same fixative and cryoprotected in 20% sucrose overnight. Cryostat sections (14 to 16 μ m) were permeabilized for 5 min in PBS containing 0.1% Triton-X, blocked for 1 h using PBS containing 10% normal goat serum and 3% bovine serum albumin, incubated with rabbit anti-PDE2A (1:100; ab14604; Abcam, Cambridge, United Kingdom) diluted in PBS containing 3% bovine serum albumin and 1% Triton-X over 2 nights at 4°C, and stained with Alexa Fluor 488- (Invitrogen/Life Technologies, Darmstadt, Germany) or Cy3 (Sigma-Aldrich)-conjugated secondary antibodies for 2 h. In double-labeling experiments, sections were then incubated with rat anti-substance P (1:200; BD Biosciences, Heidelberg, Germany), mouse anti-neuron-specific enolase (1:25; Dako, Hamburg, Germany), mouse anti-gial fibrillary acidic protein (1:1,000; Millipore, Schwalbach, Germany), rat anti-mouse CD11b (1:100; AbD Serotec/Bio-Rad, Munich, Germany), or mouse anti-caveolin-1 (1:100; Novus Biologicals, Cambridge, United Kingdom) followed by Cy3- or Alexa Fluor 555-conjugated secondary antibodies, or with Alexa Fluor 488-conjugated *Griffonia simplicifolia* isolectin B4 (IB4; 10 μ g/ml in PBS; Invitrogen/Life Technologies). After immunostaining, slides were immersed for 5 min in 0.06% Sudan black B (in 70% ethanol) to reduce lipofuscin-like autofluorescence.^{24,25} Images were taken using an Axio Observer.Z1 microscope (Carl Zeiss, Göttingen, Germany) equipped with the Zeiss Apotome oscillating grating in the epifluorescence beam, or using an Eclipse Ni microscope (Nikon, Düsseldorf, Germany).

Brightness and contrast were adjusted using Adobe Photoshop CS software (Adobe Systems, Munich, Germany).

Laser Microdissection and Real-time Reverse Transcription Polymerase Chain Reaction

Laser microdissection and real-time reverse transcription polymerase chain reaction (PCR) were performed as described in detail previously.¹² Briefly, lumbar spinal cords (L4 to L6) were dissected, cryosectioned (16 μm), stained in 1% cresyl violet solution (Sigma-Aldrich), and dehydrated through 75 to 100% ethanol. A Leica LMD6500 system (Leica Microsystems, Wetzlar, Germany) was used to collect the superficial dorsal horn (laminae I to III) and ventral horn (laminae VII to IX) separately.¹² RNA was isolated from the microdissected tissue using the RNeasy Plus Micro Kit (Qiagen, Hilden, Germany), and integrity of the isolated RNA was confirmed using the Agilent 2100 bioanalyzer and RNA 6000 Pico LabChip Kit (Agilent Technologies, Böblingen, Germany). Real-time reverse transcription PCR was performed on a 7500 Fast Real-Time PCR System (Applied Biosystems/Life Technologies, Darmstadt, Germany) using TaqMan gene expression assays for PDE2A (catalog no. Mm01136644_m1; Applied Biosystems/Life Technologies) and glyceraldehyde 3-phosphate dehydrogenase (catalog no. Mm99999915_g1; Applied Biosystems/Life Technologies). The quantity of PDE2A messenger RNA (mRNA) relative to glyceraldehyde 3-phosphate dehydrogenase mRNA was calculated by the $2^{-\Delta\Delta\text{CT}}$ method. Control experiments revealed stable glyceraldehyde 3-phosphate dehydrogenase mRNA expression levels in the dorsal and ventral horn after zymosan injection into a hind paw or after SNI.

Determination of Cyclic Nucleotides in Spinal Cord Slices

Mice were exsanguinated under deep isoflurane anesthesia, and the spinal cord was dissected and kept in cold Ringer's buffer containing 136 mM NaCl, 5.4 mM KCl, 1.8 mM CaCl_2 , 0.33 mM NaH_2PO_4 , 10 mM HEPES, and 10 mM glucose; pH 7.2. Transversal slices (600 μm) were cut on a vibratome and equilibrated in 100 μl Ringer's buffer for 1 h at room temperature. Slices were then incubated with 1 μM BAY 60-7550 or vehicle (4.8% ethanol) for 10 min at 37°C, followed by incubation with 300 μM *N*-methyl-D-aspartate²⁶ for 5 min at 37°C. Then enzymatic reactions were stopped by microwave fixation at 1,200 W for 10 s, and the slices were snap-frozen in liquid nitrogen.

For sample extraction, the slices were homogenized on ice in 110 μl cold methanol containing 1 ng of the internal standard 8-(4-chlorophenylthio)guanosine-3',5'-cyclic monophosphate (Biolog), followed by adding of 400 μl cold methanol and vortexing. Samples were analyzed by liquid chromatography–electrospray ionization–tandem mass spectrometry with a hybrid triple quadrupole–ion trap mass spectrometer model 5500 QTRAP (AB Sciex, Darmstadt, Germany) equipped with a Turbo Ion Spray source operating in negative ion mode. The coupled high-performance

liquid chromatography system consisted of an Agilent 1200 Series binary pump, degasser, and column oven connected to a CTC PAL autosampler (Chromtech, Idstein, Germany).

To obtain linear calibration curves in the range between 0.1 and 50 ng/ml, a standard stock solution of cAMP and cGMP (1,000 ng/ml in methanol; Biolog) was diluted to different working solutions in the range between 0.5 and 250 ng/ml. Twenty microliter of every working solution was mixed with 15 μl PBS (Dulbecco PBS without Ca^{2+} and Mg^{2+} ; GE Healthcare Life Sciences, Freiburg, Germany), 440 μl cold methanol, and 10 μl of the internal standard 8-(4-chlorophenylthio)guanosine-3',5'-cyclic monophosphate (100 ng/ml in methanol). The tubes were vortexed and centrifuged at 20,238g for 3.5 min. Supernatant was collected, and solvent was evaporated under nitrogen at 45°C. Standard samples were resuspended in 100 μl water and transferred to glass vials. Quality control samples were prepared the same way.

For chromatographic separation, an Atlantis T3 column (100 mm \times 2.1 mm I.D., 3 μm particle size; Waters, Eschborn, Germany) in combination with an AQ C18 guard column (4 mm, 2 mm I.D.; Phenomenex, Aschaffenburg, Germany) was used. Column oven was tempered at 40°C, and the flow rate was set at 0.3 ml/min. Samples (10 μl) were injected into the liquid chromatographic system, and analytes were eluted under gradient conditions using mobile phase A (water with 5 mM ammonium formate) and mobile phase B (methanol with 5 mM ammonium formate). The gradient program started with 100% A for 1.5 min, and within 3 min, the fraction of A was linearly decreased to 10% and remained so for 5 min. For 2 min, it was linearly increased again to 100% A, and column was reequilibrated for 3 min. From 0 to 3 min, the integrated valco valve was switched to waste.

The mass spectrometer was operated in negative multiple reaction monitoring mode with all quadrupoles running at unit resolution. Ionization source was working with an ion-spray voltage of $-4,500$ V at 450°C. The gases were set as follows: gas 1: 50 instrument units; gas 2: 60 instrument units; curtain gas: 40 instrument units; collision gas: 9 instrument units. Entrance potential was -10 V for all analytes, whereas declustering potential, collision energy, and collision cell exit potential were optimized for every substance manually. This was performed by infusing standard solutions of 50 ng/ml of the analytes into the mass spectrometer. The precursor-to-product ion transitions (m/z) used for quantification, and the declustering potential, collision energy, and collision cell exit potential values were as follows: cAMP, m/z : 328.0 \rightarrow 79.0; declustering potential: -120.0 V; collision energy: -86.5 V; collision cell exit potential: -37.0 V. cGMP, m/z : 344.0 \rightarrow 78.8; declustering potential: -65.0 V; collision energy: -78.0 V; collision cell exit potential: -37.0 V. For all transitions, a dwell time of 50 ms was set.

Statistical Analysis

All data are presented as mean \pm SEM. Statistical analysis was performed with IBM SPSS Statistics software (version 21;

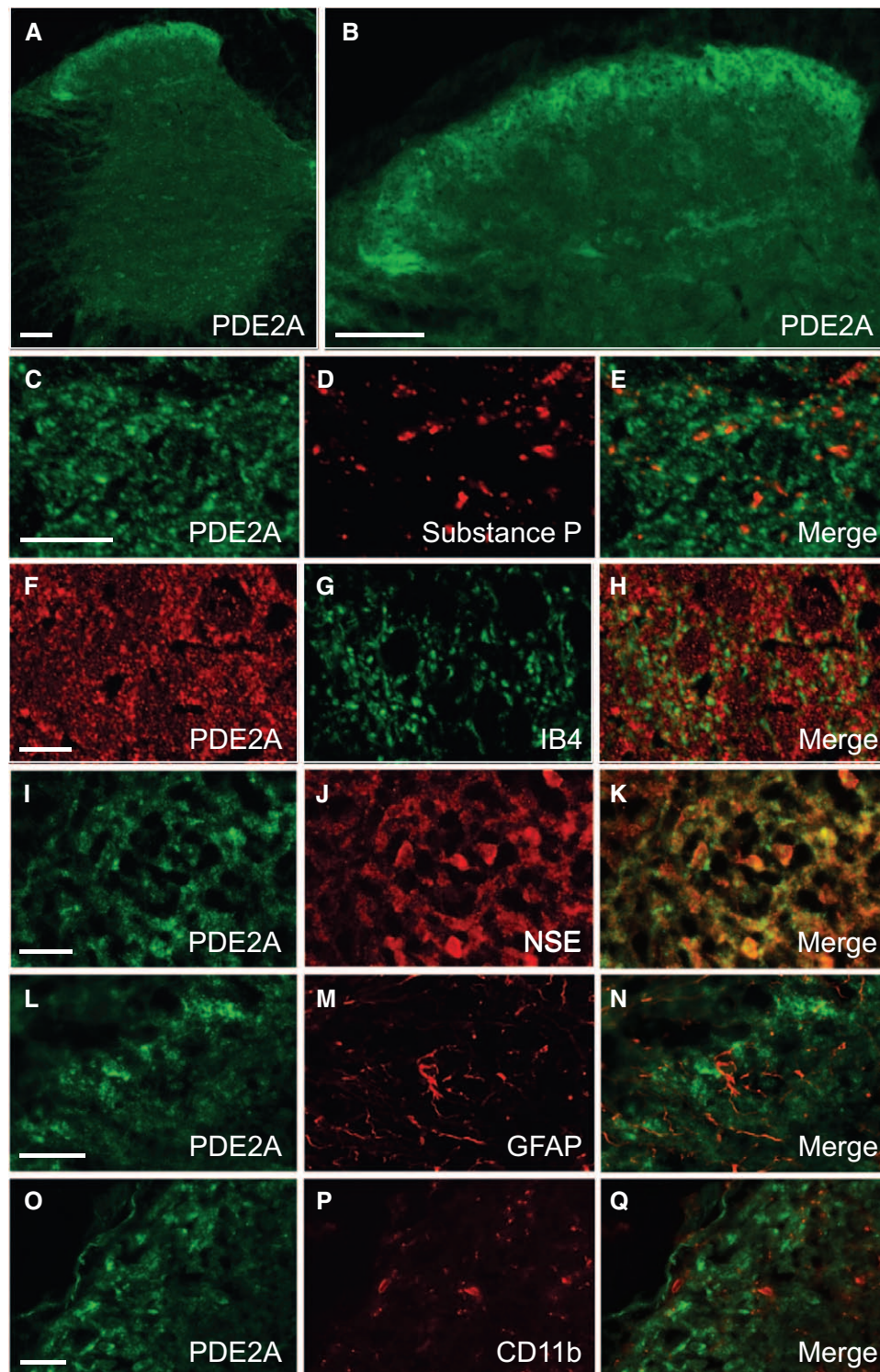


Fig. 1. Phosphodiesterase 2A (PDE2A) expression in the spinal cord. (A) PDE2A immunoreactivity is concentrated in the most superficial laminae of the dorsal horn. (B) Higher magnification of A. (C–Q) Double labeling of PDE2A and substance P (C–E), isolectin B4 (IB4; F–H), neuron-specific enolase (NSE; I–K), glial fibrillary acidic protein (GFAP; L–N), and CD11b (O–Q). Note that PDE2A is colocalized with NSE, but not with substance P, IB4, GFAP, or CD11b. Scale bars: A, B: 100 μ m; C, F: 10 μ m; I, L, O: 20 μ m.

IBM, Ehningen, Germany). Data for mRNA expression and behavioral data in the formalin test were analyzed by one-way ANOVA with Bonferroni *post hoc* test. Behavioral data in the

zymosan model, the SNI model, and after intrathecal drug injection were analyzed using a two-way repeated-measures ANOVA with Bonferroni *post hoc* test. Comparisons of two means were

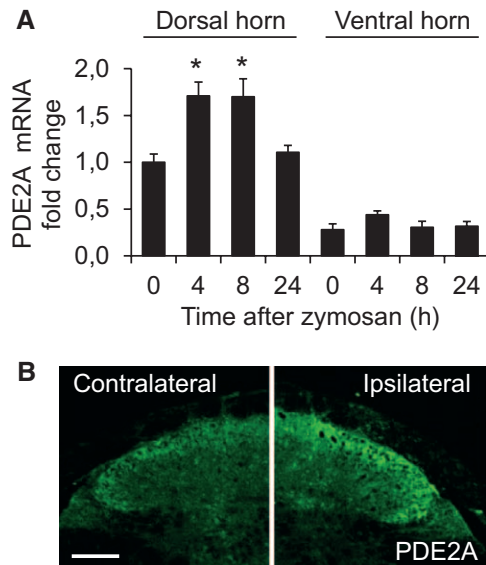


Fig. 2. Phosphodiesterase 2A (PDE2A) expression in the dorsal horn is upregulated during paw inflammation. (A) PDE2A messenger RNA (mRNA) expression in the superficial dorsal horn and ventral horn of the spinal cord after intraplantar zymosan injection. Dorsal horn (laminae I–III) and ventral horn (laminae VII–IX) sections were collected using laser microdissection, and mRNA levels were determined using quantitative real-time reverse transcription polymerase chain reaction. Data show that the intraplantar zymosan injection induced a significant upregulation of PDE2A mRNA expression in the superficial dorsal horn. $n = 3$ per group. $*P < 0.05$. (B) PDE2A protein expression in the dorsal horn of the spinal cord 8 h after intraplantar zymosan injection into one hind paw. Note that PDE2A immunoreactivity in the superficial dorsal horn is more intense at the ipsilateral, zymosan-injected side as compared with the contralateral, noninjected side. Scale bar: 100 μm .

made by unpaired two-tailed Student *t* test. For all tests, *P* values less than 0.05 were considered statistically significant.

Results

PDE2A Expression Is Enriched in the Superficial Dorsal Horn and Upregulated after Inflammatory Stimulation

First, we examined the PDE2A distribution in the mouse spinal cord by immunostaining. We observed a dense band of PDE2A immunoreactivity in the most superficial laminae of the dorsal horn (laminae I and II) and weak PDE2A immunoreactivity in some neurons in the intermediate spinal cord and the ventral horn (fig. 1, A and B), confirming the PDE2A distribution that has been detected in the rat spinal cord by using another anti-PDE2A antibody.¹⁷ To characterize the distribution of PDE2A in the superficial dorsal horn in more detail, we performed double-labeling experiments with substance P and lectin IB4, markers of nociceptive primary afferent neurons that terminate in laminae I and II, respectively. Surprisingly, there was virtually no overlap of PDE2A immunoreactivity with fibers positive for substance P (fig. 1, C–E) or IB4 (fig. 1, F–H), although

many PDE2A-immunoreactive puncta were in close proximity to puncta positive for substance P or IB4. PDE2A immunoreactivity overlapped, however, with the neuronal marker neuron-specific enolase (fig. 1, I–K). Moreover, the PDE2A staining pattern essentially differed from that of glial fibrillary acidic protein (fig. 1, L–N) and CD11b (fig. 1, O–Q), which are markers of astroglia and microglia, respectively. The overlap with a marker of neurons and the lack of colocalization with markers of primary afferent fibers and glial cells point to an expression of PDE2A in neurons of the superficial dorsal horn, that is, in cells that essentially contribute to nociceptive processing.

We then performed laser microdissection to isolate superficial dorsal horn (laminae I to III) and ventral horn (laminae VII to IX) spinal cord tissues,¹² and analyzed the PDE2A mRNA expression in the isolated tissues by quantitative real-time reverse transcription PCR. In line with the PDE2A protein distribution, we detected much higher PDE2A mRNA levels in the superficial dorsal horn compared with the ventral horn (fig. 2A). To further assess a potential contribution of PDE2A to nociceptive processing, we investigated the PDE2A mRNA expression in the dorsal and ventral horn after hind paw injection with the proinflammatory compound zymosan. Notably, the zymosan injection significantly increased the PDE2A mRNA expression in the superficial dorsal horn but not in the ventral horn (fig. 2A), further pointing to a pain-relevant function of PDE2A. The PDE2A mRNA upregulation was paralleled by an increased PDE2A immunoreactivity in the superficial dorsal horn 8 h after zymosan injection into a hind paw. However, the general PDE2A distribution pattern in the dorsal horn was similar between the zymosan-injected (ipsilateral) and the noninjected (contralateral) sides (fig. 2B), and double-labeling experiments revealed that the PDE2A upregulation occurred in neurons but not in glial cells (data not shown). We concluded that PDE2A expression in the spinal cord is upregulated in neurons of the superficial dorsal horn after intraplantar zymosan injection. Together, these data suggest a contribution of PDE2A to the processing of inflammatory pain in the spinal cord.

We next assessed the PDE2A distribution in DRGs by immunostaining. In general, PDE2A immunoreactivity was weaker in DRGs as compared with the superficial dorsal horn (fig. 3). Significant PDE2A immunoreactivity in DRGs was detected in capillary endothelial cells identified by their morphology (fig. 3, A and C) and by colocalization with the marker caveolin-1 (fig. 3, C–E). We also detected PDE2A immunoreactivity, which was however only little above background, in the somata of most DRG neurons (fig. 3, A and B). In contrast to the dorsal horn of the spinal cord, the PDE2A expression in DRGs was not significantly upregulated 4, 8, or 24 h after zymosan injection into a hind paw, as assessed by quantitative real-time reverse transcription PCR. The relative mRNA expression was 1.01 ± 0.09 (naive), 0.85 ± 0.17 (4h), 0.95 ± 0.05 (8h), and 0.99 ± 0.08 (24h), $n = 3$ per group. Considering the more prominent

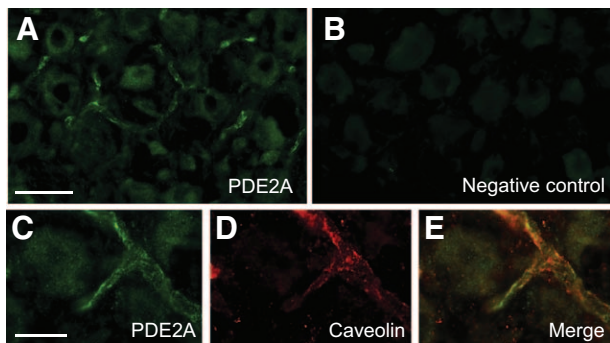


Fig. 3. Phosphodiesterase 2A (PDE2A) expression in dorsal root ganglia. (A and B) Distinct PDE2A immunoreactivity is present in capillary endothelial cells, whereas weak PDE2A immunoreactivity is detectable in neurons. The neuronal PDE2A immunoreactivity is only little above background, as compared with staining without primary antibody (B). (C–E) Double labeling of PDE2A and caveolin-1 confirms PDE2A expression in capillary endothelial cells. Scale bars: 20 μ m.

expression and zymosan-induced upregulation in neurons of the superficial dorsal horn, these data point to a limited contribution of PDE2A expressed in DRGs to the processing of inflammatory pain after intraplantar zymosan injection.

Inflammatory Pain Behaviors Are Increased after Inhibition of PDE2A

To assess whether PDE2A plays a functional role in inflammatory pain processing *in vivo*, we evaluated the effects of the selective PDE2A inhibitor, BAY 60-7550,¹⁹ on inflammatory pain behavior in mice. We first analyzed the effects of PDE2A inhibition in the formalin test, a well-characterized model of inflammatory pain.²⁰ We administered BAY 60-7550 (1, 3, and 9 mg/kg intraperitoneal) or vehicle 20 min before 5% formalin injection into a hind paw and observed the nociceptive behavior during 45 min. The formalin injection evoked the typical biphasic paw-licking behavior. The first phase of paw licking (1 to 10 min), which mainly depends on peripheral activation of primary afferent neurons,²⁷ was not affected by BAY 60-7550 pretreatment (fig. 4A). Interestingly however, BAY 60-7550 at doses of 3 and 9 mg/kg significantly increased the second phase of paw licking (11 to 45 min; fig. 4A). Considering that the second phase of paw licking involves a period of central sensitization in the dorsal horn of the spinal cord,²⁷ and that BAY 60-7550 at doses of 3 mg/kg or greater crosses the blood–brain barrier,^{19,28,29} these data point to a central (*i.e.*, spinal cord mediated) rather than a peripheral mechanism accounting for the pronociceptive effects of BAY 60-7550.

We then assessed the effect of 3 mg/kg BAY 60-7550 (*i.e.*, a dose that was pronociceptive in the formalin test) in the intraplantar zymosan assay, another model of inflammatory pain.³⁰ Injection of zymosan into a hind paw induced a mechanical hypersensitivity of the injected paw (fig. 4B), as expected. Four hours after zymosan injection, we intraperitoneally administered BAY 60-7550 or vehicle. Interestingly,

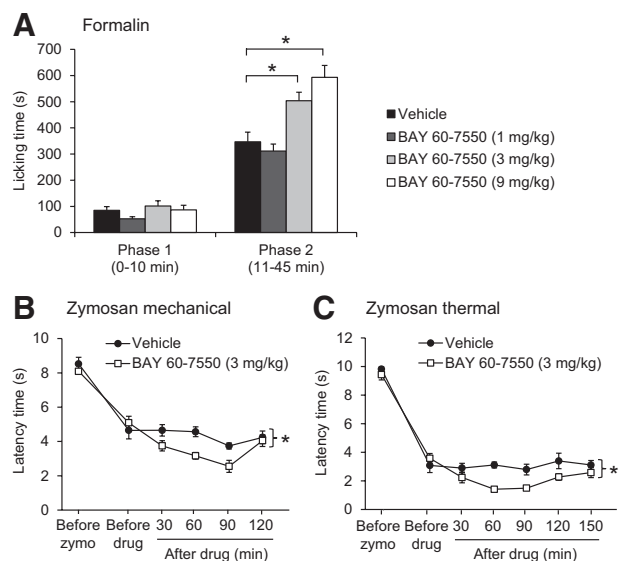


Fig. 4. Increased inflammatory pain behavior after phosphodiesterase 2A inhibition. (A) Formalin test. Drugs (1, 3, and 9 mg/kg BAY 60-7550, or vehicle) were intraperitoneally administered 20 min before injection of 5% formalin into a hind paw. Sum of paw-licking time in phase 1 (1–10 min) and phase 2 (11–45 min) after formalin injection. $n = 10$ per group for vehicle and 3 mg/kg BAY 60-7550, $n = 8$ per group for 1 and 9 mg/kg BAY 60-7550; $*P < 0.05$. (B and C) Zymosan model. Mice were tested for (B) mechanical and (C) thermal paw sensitivity before zymosan injection into a hind paw (“before zymo”) and 4 h thereafter (“before drug”). Then drugs (3 mg/kg BAY 60-7550 or vehicle) were intraperitoneally administered, and the paw sensitivity was determined. $n = 6$ per group; $*P < 0.05$, representing group main effects. Note that the paw-licking behavior in phase 2 (A) and the mechanical and thermal paw hypersensitivities (B and C) were significantly increased in mice treated with 3 or 9 mg/kg BAY 60-7550.

BAY 60-7550 significantly increased the mechanical hypersensitivity as compared with vehicle-treated animals (fig. 4B). Two-way repeated-measures ANOVA revealed a significant effect of the group ($P = 0.035$), time ($P < 0.001$), and their interaction ($P = 0.031$). Similarly, the thermal hypersensitivity that developed after zymosan injection was increased after administration of BAY 60-7550 (fig. 4C). The effect of group ($P = 0.035$) and time ($P = 0.006$) was significant, whereas group \times time effects were not significant ($P = 0.181$). In control experiments, we examined the effects of BAY 60-7550 (3 mg/kg intraperitoneal) on paw-withdrawal latencies in naive animals, that is, in the absence of paw inflammation. One hour after administration of BAY 60-7550, neither mechanical (fig. 5A) nor thermal (fig. 5B) paw-withdrawal latencies were significantly altered as compared with vehicle, indicating that the baseline sensitivity to noxious mechanical and thermal stimuli was not affected by the PDE2A inhibitor. Altogether, these data demonstrate that PDE2A is functionally involved in the processing of inflammatory pain induced by paw inflammation.

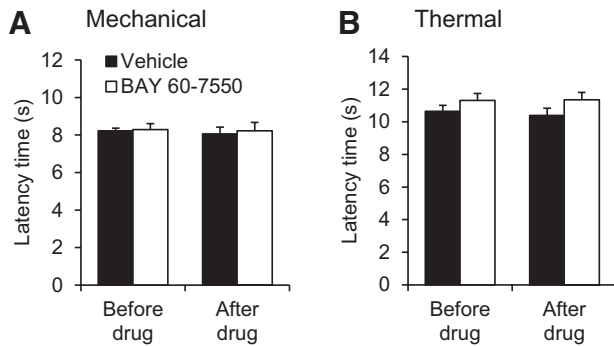


Fig. 5. Limited effect of phosphodiesterase 2A inhibition on acute nociceptive behavior. Mice were tested for (A) mechanical and (B) thermal paw sensitivity before and 60 min after drug administration (3 mg/kg BAY 60–7550 or vehicle intraperitoneal; $n = 6$ per group). The acute nociceptive behavior was not affected by BAY 60–7550 in both tests.

PDE2A Inhibition Increases Spinal Pronociceptive Effects of cAMP

PDE2A is a dual-substrate enzyme able to hydrolyze both cAMP and cGMP. To assess whether one, or both, of these cyclic nucleotides contributes to the PDE2A-modulated processing of pain in the spinal cord, we analyzed the effects of systemic PDE2A inhibition on the paw hypersensitivity evoked by intrathecal delivery of cyclic nucleotides. Mice were intraperitoneally administered with BAY 60–7550 (3 mg/kg) or vehicle, and cyclic nucleotides were intrathecally injected 1 h thereafter. After intrathecal injection of cAMP (40 nmol), paw-withdrawal latencies were decreased in both groups, indicating the mice developed mechanical hypersensitivity (fig. 6A). However, the extent of cAMP-induced mechanical hypersensitivity was significantly increased in mice pretreated with BAY 60–7550 as compared with those pretreated with vehicle (fig. 6A). Two-way repeated-measures ANOVA revealed significant group ($P = 0.041$) and group \times time ($P = 0.032$) effects. Similarly, the mechanical hypersensitivity evoked by intrathecal injection of the cAMP analog, Sp-8-Br-cAMPS (20 nmol), was increased after pretreatment with BAY 60–7550 (group effect: $P = 0.013$, group \times time effect: $P = 0.003$; fig. 6B). In contrast, intraperitoneal pretreatment with BAY 60–7550 did not significantly affect the mechanical hypersensitivity induced by intrathecal injection of cGMP (40 nmol; group effect: $P = 0.804$; fig. 6C) or that induced by intrathecal injection of the nitric oxide donor NOC-5 (10 μ g; group effect: $P = 0.373$; fig. 6D), which increases the cGMP production in the spinal cord after activation of nitric oxide-sensitive guanylyl cyclase (also termed soluble guanylyl cyclase).³¹ These data suggest that pronociceptive pathways involving cAMP, but not cGMP, are modulated by PDE2A in the spinal cord.

We next assessed whether BAY 60–7550 treatment increases the cyclic nucleotide concentration in the spinal cord. For that purpose, we incubated acute slices of the

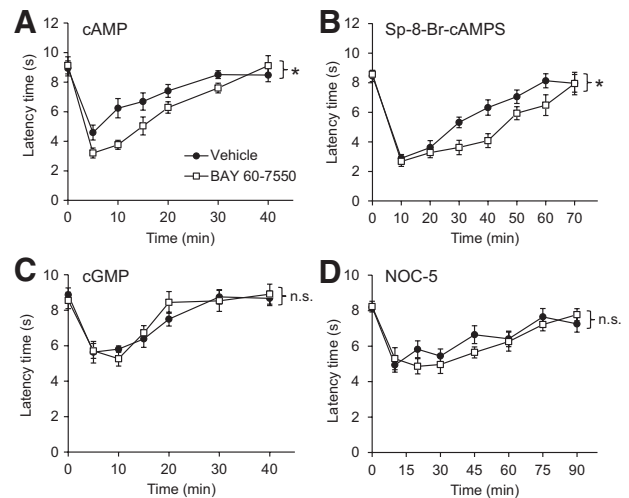


Fig. 6. Phosphodiesterase 2A in the spinal cord modulates hypersensitivity induced by cyclic adenosine monophosphate (cAMP). Time course of mechanical hypersensitivity induced by intrathecal administration of cAMP (40 nmol; $n = 8$; A), the cAMP analog Sp-8-Br-cAMPS (20 nmol; $n = 8$; B), cyclic guanosine monophosphate (cGMP; 40 nmol; $n = 6$; C), or the nitric oxide donor NOC-5 (10 μ g; $n = 8$; D). One hour before intrathecal drug delivery, mice were intraperitoneally pretreated with 3 mg/kg BAY 60–7550 or vehicle. Data indicate that the BAY 60–7550 pretreatment increased the extent of hypersensitivity induced by cAMP or Sp-8-Br-cAMPS ($*P < 0.05$, representing group main effects) but not the hypersensitivity evoked by cGMP or NOC-5. n.s. = not significant.

mouse spinal cord with BAY 60–7550 or vehicle, stimulated cyclic nucleotide production with *N*-methyl-D-aspartate,²⁶ and measured the cAMP and cGMP levels by liquid chromatography–electrospray ionization–tandem mass spectrometry. Notably, BAY 60–7550 significantly increased the cAMP levels in the spinal cord slices as compared with vehicle (fig. 7). In contrast to cAMP, the cGMP levels could not be detected in our analyses because they were below the lower limit of quantification (0.125 ng/ml for both cAMP and cGMP). Altogether, these data indicate that PDE2A contributes to the degradation of cAMP in the spinal cord.

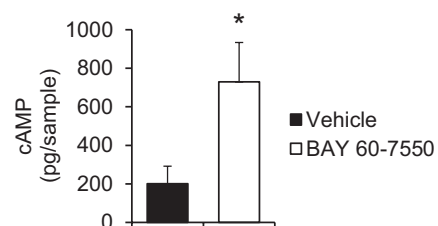


Fig. 7. Increased cyclic adenosine monophosphate (cAMP) levels in the spinal cord after phosphodiesterase 2A inhibition. Spinal cord slices were preincubated with BAY 60–7550 (1 μ M) or vehicle, and stimulated with *N*-methyl-D-aspartate (300 μ M). Note that the BAY 60–7550 pretreatment increased the cAMP levels. $n = 7$ per group. $*P < 0.05$.

Neuropathic Pain Behavior after Peripheral Nerve Injury Is Not Affected by PDE2A Inhibition

Finally, we investigated whether neuropathic pain processing is modulated by inhibition of PDE2A. Mice were subjected to SNI, which induced a mechanical hypersensitivity of the affected hind paw 14 days after surgery. In contrast to the inflammatory pain behavior during paw inflammation, the SNI-induced neuropathic pain behavior was not significantly affected by administration of BAY 60–7550 (3 mg/kg intraperitoneal; group effect: $P = 0.426$; fig. 8A). Moreover, unlike the zymosan-induced upregulation, PDE2A mRNA was not upregulated in the dorsal horn of the spinal cord after SNI (fig. 8B). Thus, PDE2A does not seem to be critically involved in the processing of neuropathic pain after peripheral nerve injury.

Discussion

Here, we demonstrate that PDE2A in the spinal cord exerts pain-relevant functions *in vivo*. PDE2A expression in the dorsal horn of the spinal cord is upregulated during paw inflammation in mice. Their nociceptive behavior after administration of a PDE2A inhibitor suggests that PDE2A functionally contributes to the processing of inflammatory pain associated with paw inflammation, and that PDE2A modulates pronociceptive effects of cAMP. On the contrary, PDE2A does not seem to affect neuropathic pain processing after peripheral nerve injury.

Previous studies revealed that PDE2A is expressed in a wide variety of tissues, with the highest expression levels found in the brain and lower levels in endothelial cells of most tissues, platelets, the adrenal zona glomerulosa, enteric ganglia, and lymphoid organs. Similar expression patterns have been found across several mammalian species, from human to macaque to dogs and rodents, arguing for an evolutionary conserved function of PDE2A.^{17,32} Given that PDE2A is present in many cell types and has the ability to hydrolyze both cAMP and cGMP with high activity, it is conceivable that it regulates a variety of different processes.¹⁸ In fact, PDE2A has been reported to be involved in various functions, including learning and enhancement of neuronal plasticity,^{33–35} blunting of anxiety,²⁸ excitation–contraction coupling and compartmentation of cyclic nucleotide signaling in cardiomyocytes,^{36,37} endothelial cell permeability,^{38,39} angiogenesis,⁴⁰ platelet aggregation,⁴¹ and aldosterone production.^{42,43} Dependent on the vicinity of PDE2A to generators and downstream effectors of cyclic nucleotides, inhibition of PDE2A in any of these cells can result in elevation of cAMP, cGMP, or both.¹⁶

Here, we provide several lines of evidence for a to date unrecognized contribution of PDE2A to pain processing in the superficial dorsal horn of the spinal cord. First, PDE2A is distinctly expressed in neurons of the superficial dorsal horn, and its expression in the superficial dorsal horn is upregulated after induction of paw inflammation using zymosan. The fact that proinflammatory stimuli may increase the expression of PDE2A is supported by reports demonstrating increased PDE2A mRNA levels in the spinal cord after

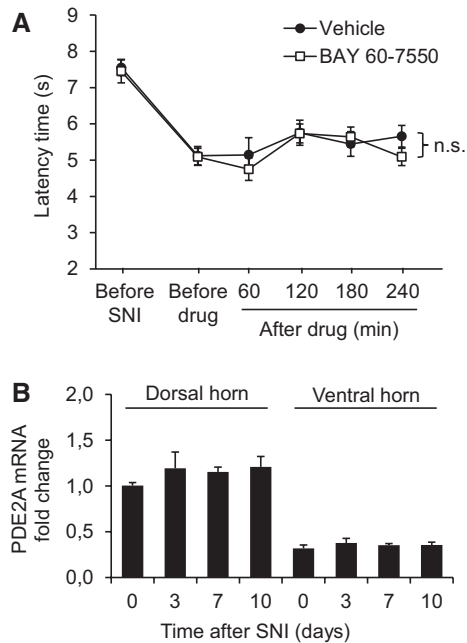


Fig. 8. Limited effect of phosphodiesterase 2A (PDE2A) inhibition on spared nerve injury (SNI)-induced neuropathic pain processing. (A) Mice were tested for mechanical paw sensitivity before SNI and 14 days thereafter (“before drug”). Then drugs (3 mg/kg BAY 60–7550, $n = 6$; or vehicle, $n = 5$) were intraperitoneally administered, and the paw sensitivity was determined. The neuropathic pain behavior was not affected by BAY 60–7550. (B) PDE2A messenger RNA (mRNA) expression in the superficial dorsal horn (laminae I–III) and ventral horn (laminae VII–IX) of the spinal cord after SNI. Dorsal and ventral horn sections were collected using laser microdissection, and mRNA levels were determined using quantitative real-time reverse transcription polymerase chain reaction. $n = 3$ per group. Data show that PDE2A mRNA expression did not change after SNI. n.s. = not significant.

formalin injection into a hind paw,⁴⁴ in cultured endothelial cells stimulated with tumor necrosis factor- α ,³⁸ and in cultured peritoneal macrophages after incubation with lipopolysaccharide.⁴⁵ Second, the inflammatory pain behavior in the formalin and zymosan model was increased after administration of the selective PDE2A inhibitor, BAY 60–7550. This compound is more than 100-fold more potent than the “classical” PDE2A inhibitor, erythro-9-(2-hydroxy-3-nonyl)adenine, which also inhibits adenosine deaminase.¹⁶ We found that BAY 60–7550 increased the inflammatory pain behavior at doses that affected brain functions in earlier studies (≥ 3 mg/kg),^{19,28,29} providing further evidence that BAY 60–7550 crosses the blood–brain barrier and may affect PDE2A localized in the spinal cord. This assumption is further supported by the fact that the second (central) but not the first (peripheral) phase in the formalin test was modulated by pretreatment with BAY 60–7550. Third, the immediate pain behaviors evoked by spinal delivery of cAMP and Sp-8-Br-cAMPS were increased after systemic pretreatment with BAY 60–7550, whereas those evoked by spinal delivery

of cGMP and NOC-5 were not affected. Finally, cAMP levels in spinal cord slices were increased in the presence of BAY 60–7550. Hence, our data imply that PDE2A in the superficial dorsal horn is functionally involved in the processing of inflammatory pain induced by paw inflammation and in the degradation of cAMP. We can, however, not exclude the possibility that PDE2A expressed in DRG neurons also contributes to pain processing. Our observations that PDE2A immunoreactivity seems much more intense in dorsal horn neurons as compared with DRG neurons, and that intraplantar zymosan induces upregulation of PDE2A expression in the dorsal horn but not in DRGs, argue against an important function of PDE2A in DRG neurons during the processing of inflammatory pain induced by paw inflammation.

In contrast to the inflammatory pain behavior, treatment with BAY 60–7550 did not affect the neuropathic pain behavior after SNI. This observation is in line with earlier reports, in which knockout or pharmacological modulation of a target only affected the behavior in animal models of inflammatory pain or neuropathic pain, but not both.^{12,21,25,46} The causes of inflammatory pain and neuropathic pain are fundamentally different, and both principal pain categories can be distinguished from several characteristics, such as resolution of pain as a function of “healing” (characteristic of inflammatory pain), involvement of A β afferents in addition to C fibers (characteristic of neuropathic pain), and sensitivity to pharmacological treatment.⁴⁷ However, there are also common mechanisms underlying the generation of each pain state. These mechanisms include, for example, glia activation and disinhibition in the spinal dorsal horn, as well as immune cell invasion and release of proinflammatory compounds in peripheral tissues.⁴⁷ Notably, several neuropathic pain states, including neuropathy after peripheral nerve injury, are in themselves associated with peripheral inflammation, which might contribute to the pain processing.⁴⁸ The complex pathological conditions and the peripheral and spinal mechanisms underlying neuropathic pain await further analyses. However, our data suggest that PDE2A is not critically involved in the pain processing after peripheral nerve injury.

A recent study reported the synthesis of new, orally bioavailable selective PDE2A inhibitors that are nonbrain penetrant.⁴⁹ One of these inhibitors, compound 22, ameliorated osteoarthritis pain in rats. To the best of our knowledge, it is currently unknown which peripheral cells mediate this pain-relevant effect of PDE2A. However, the antinociceptive effect of peripherally restricted PDE2A inhibition is in distinct contrast to the pronociceptive effect of PDE2A inhibition in the spinal cord. Considering the widespread distribution of PDE2A in different cells and the fact that its precise intracellular localization is crucial for control of cAMP and/or cGMP signaling, it is likely that PDE2A, dependent on its localization, may exert both anti- and pronociceptive effects. One important conclusion is that blood–brain penetration must be prevented if PDE2A inhibitors are used for treatment

of inflammatory pain states. On the contrary, inhibition of PDE2A activity in the brain has recently gained increased attention as a potential therapeutic target to improve cognition associated with neuropsychiatric disorders, such as schizophrenia and Alzheimer’s disease.^{29,50,51} Because these drugs reach the central nervous system, including the spinal cord, they should be carefully tested in light of possible side effects in patients with inflammatory pain as a comorbidity.

In conclusion, we have presented evidence for an inhibitory role of PDE2A for the processing of inflammatory pain in the spinal cord. It remains to be determined which other PDEs are involved in nociceptive processing and terminate pro- and/or antinociceptive effects of cyclic nucleotides.

Acknowledgments

The authors thank Christine Manderscheid, Karin Schilling, and Judith Fuchs (Institut für Klinische Pharmakologie, Universitätsklinikum Frankfurt, Frankfurt am Main, Germany), Natalie Wolfsdorff (Institut für Pharmakologie und Toxikologie, Universität Witten/Herdecke, Witten, Germany), and Heike Korff (Institut für Klinische Neuroanatomie, Goethe-Universität, Frankfurt am Main, Germany) for excellent technical assistance.

This work was supported by the Deutsche Forschungsgemeinschaft, Bonn, Germany (grant no. SFB815-A14), and the Interdisciplinary Center for Neuroscience Frankfurt, Frankfurt, Germany.

Competing Interests

The authors declare no competing interests.

Correspondence

Address correspondence to Dr. Schmidtko: Institut für Pharmakologie und Toxikologie, Zentrum für Biomedizinische Ausbildung und Forschung, Universität Witten/Herdecke, Stockumer Str. 10, 58453 Witten, Germany. achim.schmidtko@uni-wh.de. Information on purchasing reprints may be found at www.anesthesiology.org or on the masthead page at the beginning of this issue. ANESTHESIOLOGY’s articles are made freely accessible to all readers, for personal use only, 6 months from the cover date of the issue.

References

1. Basbaum AI, Bautista DM, Scherrer G, Julius D: Cellular and molecular mechanisms of pain. *Cell* 2009; 139:267–84
2. Malmberg AB, Brandon EP, Idzerda RL, Liu H, McKnight GS, Basbaum AI: Diminished inflammation and nociceptive pain with preservation of neuropathic pain in mice with a targeted mutation of the type I regulatory subunit of cAMP-dependent protein kinase. *J Neurosci* 1997; 17:7462–70
3. Aley KO, Levine JD: Role of protein kinase A in the maintenance of inflammatory pain. *J Neurosci* 1999; 19:2181–6
4. Ahmadi S, Lippross S, Neuhuber WL, Zeilhofer HU: PGE(2) selectively blocks inhibitory glycinergic neurotransmission onto rat superficial dorsal horn neurons. *Nat Neurosci* 2002; 5:34–40
5. Bhawe G, Zhu W, Wang H, Brasier DJ, Oxford GS, Gereau RW IV: cAMP-dependent protein kinase regulates desensitization of the capsaicin receptor (VR1) by direct phosphorylation. *Neuron* 2002; 35:721–31
6. Hucho TB, Dina OA, Levine JD: Epac mediates a cAMP-to-PKC signaling in inflammatory pain: An isolectin B4(+) neuron-specific mechanism. *J Neurosci* 2005; 25:6119–26

7. Eijkelkamp N, Linley JE, Torres JM, Bee L, Dickenson AH, Gringhuis M, Minett MS, Hong GS, Lee E, Oh U, Ishikawa Y, Zwartkuis FJ, Cox JJ, Wood JN: A role for Piezo2 in EPAC1-dependent mechanical allodynia. *Nat Commun* 2013; 4:1682
8. Tao YX, Johns RA: Activation of cGMP-dependent protein kinase I α is required for *N*-methyl-D-aspartate- or nitric oxide-produced spinal thermal hyperalgesia. *Eur J Pharmacol* 2000; 392:141–5
9. Tegeder I, Del Turco D, Schmidtko A, Sausbier M, Feil R, Hofmann F, Deller T, Ruth P, Geisslinger G: Reduced inflammatory hyperalgesia with preservation of acute thermal nociception in mice lacking cGMP-dependent protein kinase I. *Proc Natl Acad Sci U S A* 2004; 101:3253–7
10. Schmidtko A, Ruth P, Geisslinger G, Tegeder I: Inhibition of cyclic guanosine 5'-monophosphate-dependent protein kinase I (PKG-I) in lumbar spinal cord reduces formalin-induced hyperalgesia and PKG upregulation. *Nitric Oxide* 2003; 8:89–94
11. Luo C, Gangadharan V, Bali KK, Xie RG, Agarwal N, Kurejova M, Tappe-Theodor A, Tegeder I, Feil S, Lewin G, Polgar E, Todd AJ, Schlossmann J, Hofmann F, Liu DL, Hu SJ, Feil R, Kuner T, Kuner R: Presynaptically localized cyclic GMP-dependent protein kinase 1 is a key determinant of spinal synaptic potentiation and pain hypersensitivity. *PLoS Biol* 2012; 10:e1001283
12. Heine S, Michalakakis S, Kallenborn-Gerhardt W, Lu R, Lim HY, Weiland J, Del Turco D, Deller T, Tegeder I, Biel M, Geisslinger G, Schmidtko A: CNGA3: A target of spinal nitric oxide/cGMP signaling and modulator of inflammatory pain hypersensitivity. *J Neurosci* 2011; 31:11184–92
13. Emery EC, Young GT, Berrococo EM, Chen L, McNaughton PA: HCN2 ion channels play a central role in inflammatory and neuropathic pain. *Science* 2011; 333:1462–6
14. Schmidtko A, Tegeder I, Geisslinger G: No NO, no pain? The role of nitric oxide and cGMP in spinal pain processing. *Trends Neurosci* 2009; 32:339–46
15. Pierre S, Eschenhagen T, Geisslinger G, Scholich K: Capturing adenyl cyclases as potential drug targets. *Nat Rev Drug Discov* 2009; 8:321–35
16. Francis SH, Blount MA, Corbin JD: Mammalian cyclic nucleotide phosphodiesterases: Molecular mechanisms and physiological functions. *Physiol Rev* 2011; 91:651–90
17. Stephenson DT, Coskran TM, Kelly MP, Kleiman RJ, Morton D, O'Neill SM, Schmidt CJ, Weinberg RJ, Menniti FS: The distribution of phosphodiesterase 2A in the rat brain. *Neuroscience* 2012; 226:145–55
18. Bender AT, Beavo JA: Cyclic nucleotide phosphodiesterases: Molecular regulation to clinical use. *Pharmacol Rev* 2006; 58:488–520
19. Boess FG, Hendrix M, van der Staay FJ, Erb C, Schreiber R, van Staveren W, de Vente J, Prickaerts J, Blokland A, Koenig G: Inhibition of phosphodiesterase 2 increases neuronal cGMP, synaptic plasticity and memory performance. *Neuropharmacology* 2004; 47:1081–92
20. Hunskaar S, Fasmer OB, Hole K: Formalin test in mice, a useful technique for evaluating mild analgesics. *J Neurosci Methods* 1985; 14:69–76
21. Kallenborn-Gerhardt W, Schröder K, Del Turco D, Lu R, Kynast K, Kosowski J, Niederberger E, Shah AM, Brandes RP, Geisslinger G, Schmidtko A: NADPH oxidase-4 maintains neuropathic pain after peripheral nerve injury. *J Neurosci* 2012; 32:10136–45
22. Lu R, Schmidtko A: Direct intrathecal drug delivery in mice for detecting *in vivo* effects of cGMP on pain processing. *Methods Mol Biol* 2013; 1020:215–21
23. Decosterd I, Woolf CJ: Spared nerve injury: An animal model of persistent peripheral neuropathic pain. *Pain* 2000; 87:149–58
24. Schnell SA, Staines WA, Wessendorf MW: Reduction of lipofuscin-like autofluorescence in fluorescently labeled tissue. *J Histochem Cytochem* 1999; 47:719–30
25. Schmidtko A, Gao W, Sausbier M, Rauhmeier I, Sausbier U, Niederberger E, Scholich K, Huber A, Neuhuber W, Allescher HD, Hofmann F, Tegeder I, Ruth P, Geisslinger G: Cysteine-rich protein 2, a novel downstream effector of cGMP/cGMP-dependent protein kinase I-mediated persistent inflammatory pain. *J Neurosci* 2008; 28:1320–30
26. Taqatqeh F, Mergia E, Neitz A, Eysel UT, Koesling D, Mittmann T: More than a retrograde messenger: Nitric oxide needs two cGMP pathways to induce hippocampal long-term potentiation. *J Neurosci* 2009; 29:9344–50
27. Vardeh D, Wang D, Costigan M, Lazarus M, Saper CB, Woolf CJ, Fitzgerald GA, Samad TA: COX2 in CNS neural cells mediates mechanical inflammatory pain hypersensitivity in mice. *J Clin Invest* 2009; 119:287–94
28. Masood A, Huang Y, Hajjhussein H, Xiao L, Li H, Wang W, Hamza A, Zhan CG, O'Donnell JM: Anxiolytic effects of phosphodiesterase-2 inhibitors associated with increased cGMP signaling. *J Pharmacol Exp Ther* 2009; 331:690–9
29. Rodefer JS, Saland SK, Eckrich SJ: Selective phosphodiesterase inhibitors improve performance on the ED/ID cognitive task in rats. *Neuropharmacology* 2012; 62:1182–90
30. Meller ST, Gebhart GF: Intraplantar zymosan as a reliable, quantifiable model of thermal and mechanical hyperalgesia in the rat. *Eur J Pain* 1997; 1:43–52
31. Schmidtko A, Gao W, König P, Heine S, Motterlini R, Ruth P, Schlossmann J, Koesling D, Niederberger E, Tegeder I, Friebe A, Geisslinger G: cGMP produced by NO-sensitive guanylyl cyclase essentially contributes to inflammatory and neuropathic pain by using targets different from cGMP-dependent protein kinase I. *J Neurosci* 2008; 28:8568–76
32. Stephenson DT, Coskran TM, Wilhelms MB, Adamowicz WO, O'Donnell MM, Muravnick KB, Menniti FS, Kleiman RJ, Morton D: Immunohistochemical localization of phosphodiesterase 2A in multiple mammalian species. *J Histochem Cytochem* 2009; 57:933–49
33. van Donkelaar EL, Rutten K, Blokland A, Akkerman S, Steinbusch HW, Prickaerts J: Phosphodiesterase 2 and 5 inhibition attenuates the object memory deficit induced by acute tryptophan depletion. *Eur J Pharmacol* 2008; 600:98–104
34. Rutten K, Van Donkelaar EL, Ferrington L, Blokland A, Bollen E, Steinbusch HW, Kelly PA, Prickaerts JH: Phosphodiesterase inhibitors enhance object memory independent of cerebral blood flow and glucose utilization in rats. *Neuropsychopharmacology* 2009; 34:1914–25
35. Schmidt CJ: Phosphodiesterase inhibitors as potential cognition enhancing agents. *Curr Top Med Chem* 2010; 10:222–30
36. Fischmeister R, Castro LR, Abi-Gerges A, Rochais F, Jurevicus J, Leroy J, Vandecasteele G: Compartmentation of cyclic nucleotide signaling in the heart: The role of cyclic nucleotide phosphodiesterases. *Circ Res* 2006; 99:816–28
37. Mika D, Leroy J, Vandecasteele G, Fischmeister R: PDEs create local domains of cAMP signaling. *J Mol Cell Cardiol* 2012; 52:323–9
38. Seybold J, Thomas D, Witzenthalm M, Boral S, Hocke AC, Bürger A, Hatzelmann A, Tenor H, Schudt C, Krüll M, Schütte H, Hippenstiel S, Suttorp N: Tumor necrosis factor- α dependent expression of phosphodiesterase 2: Role in endothelial hyperpermeability. *Blood* 2005; 105:3569–76
39. Surapisitchat J, Jeon KI, Yan C, Beavo JA: Differential regulation of endothelial cell permeability by cGMP *via* phosphodiesterases 2 and 3. *Circ Res* 2007; 101:811–8
40. Diebold I, Djordjevic T, Petry A, Hatzelmann A, Tenor H, Hess J, Görlach A: Phosphodiesterase 2 mediates redox-sensitive endothelial cell proliferation and angiogenesis by thrombin *via* Rac1 and NADPH oxidase 2. *Circ Res* 2009; 104:1169–77
41. Gresele P, Momi S, Falcinelli E: Anti-platelet therapy: Phosphodiesterase inhibitors. *Br J Clin Pharmacol* 2011; 72:634–46
42. MacFarland RT, Zelus BD, Beavo JA: High concentrations of a cGMP-stimulated phosphodiesterase mediate ANP-induced

- decreases in cAMP and steroidogenesis in adrenal glomerulosa cells. *J Biol Chem* 1991; 266:136–42
43. Nikolaev VO, Gambaryan S, Engelhardt S, Walter U, Lohse MJ: Real-time monitoring of the PDE2 activity of live cells: Hormone-stimulated cAMP hydrolysis is faster than hormone-stimulated cAMP synthesis. *J Biol Chem* 2005; 280:1716–9
 44. Shi X, Li X, Clark JD: Formalin injection causes a coordinated spinal cord CO/NO-cGMP signaling system response. *Mol Pain* 2005; 1:33
 45. Witwicka H, Kobińska M, Siednienko J, Mitkiewicz M, Gorczyca WA: Expression and activity of cGMP-dependent phosphodiesterases is up-regulated by lipopolysaccharide (LPS) in rat peritoneal macrophages. *Biochim Biophys Acta* 2007; 1773:209–18
 46. Kallenborn-Gerhardt W, Lu R, Syhr KM, Heidler J, von Melchner H, Geisslinger G, Bangsow T, Schmidtke A: Antioxidant activity of sestrin 2 controls neuropathic pain after peripheral nerve injury. *Antioxid Redox Signal* 2013; 19:2013–23
 47. Xu Q, Yaksh TL: A brief comparison of the pathophysiology of inflammatory *versus* neuropathic pain. *Curr Opin Anaesthesiol* 2011; 24:400–7
 48. Ellis A, Bennett DL: Neuroinflammation and the generation of neuropathic pain. *Br J Anaesth* 2013; 111:26–37
 49. Plummer MS, Cornicelli J, Roark H, Skalitzky DJ, Stankovic CJ, Bove S, Pandit J, Goodman A, Hicks J, Shahripour A, Beidler D, Lu XK, Sanchez B, Whitehead C, Sarver R, Braden T, Gowan R, Shen XQ, Welch K, Ogden A, Sadagopan N, Baum H, Miller H, Banotai C, Spessard C, Lightle S: Discovery of potent selective bioavailable phosphodiesterase 2 (PDE2) inhibitors active in an osteoarthritis pain model. Part II: Optimization studies and demonstration of *in vivo* efficacy. *Bioorg Med Chem Lett* 2013; 23:3443–7
 50. Sierksma AS, Rutten K, Sydlik S, Rostamian S, Steinbusch HW, van den Hove DL, Prickaerts J: Chronic phosphodiesterase type 2 inhibition improves memory in the APP^{swe}/PS1^{dE9} mouse model of Alzheimer's disease. *Neuropharmacology* 2013; 64:124–36
 51. Reneerkens OA, Rutten K, Bollen E, Hage T, Blokland A, Steinbusch HW, Prickaerts J: Inhibition of phosphodiesterase type 2 or type 10 reverses object memory deficits induced by scopolamine or MK-801. *Behav Brain Res* 2013; 236:16–22